Supplementary Information (SI) for Journal of Materials Chemistry A.

Supporting Information

Rapid fabrication of selective barriers through layer-by-layer self-assembly of non-stoichiometric polyelectrolyte complexes for salt and dye fractionation

[a,b]Urvashi S. Joshi and [a,b]Suresh K. Jewrajka*

[a]Membrane Science and Separation Technology Division, Central Salt and Marine Chemicals Research Institute (CSIR-CSMCRI), G. B. Marg, Bhavnagar, Gujarat-364002, India

[b]Academy of Scientific and Innovative Research (AcSIR), Ghaziabad-201002, India

***Corresponding author**

Suresh K. Jewrajka

Email: skjewrajka@csmcri.res.in

Table of contents

Experimental Section

Materials

Poly(vinylidene fluoride) (PVDF, Solef 1015, Solvay, 2.38x10^5 g mol^{-1}) and Poly(vinylpolypyrrolidone) (PVP, Aldrich, 3.6x10^5 g mol^{-1}) were used as received. 4-vinylbenzyl chloride (VBC), methyl methacrylate (MMA), trimethylamine (NMe_3), sodium 4-styrenesulfonate ($StSO_3Na$) and vinyl imidazole (VIm) were purchased from TCI Chemicals. The liquid monomers were passed through aluminium column twice prior to the polymerization. 4,4′-azobis(4-cyanovaleric acid) (ACPA) and azobisisobutyronitrile (AIBN) were from Aldrich. Polyethylene glycol (PEG) and polyethylene oxide (PEO) were from Aldrich. NaCl, Na_2SO_4 and $MgCl_2$ were from Fisher Scientific. The dyes Congo red (CR), Direct red-80 (DR-80), Rose Bengal (RB), Reactive black-5 (RB-5), Omega chrome black blue G (OG) and Acid orange-7 (AO-7) were from TCI Chemicals. The molecular structure, molecular weight, charge, and size of the dyes are depicted in Table S1.

Molecular structure and molecualr weight (g mol^{-1}) of dyes	Charge	Size (nm)[1-3]
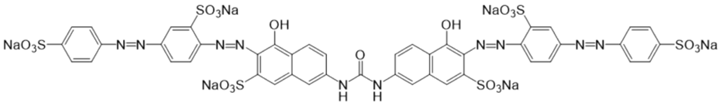 Direct red 80 (DR-80) Molecular weight: 1373	Negative	4.4
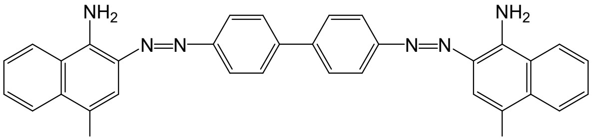 Congo red (CR) Molecular weight: 696.7	Negative	2.5
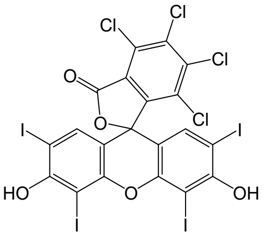 Rose Bengal (RB) Molecular weight: 1,017.6 (sodium salt)	Negative	1.58
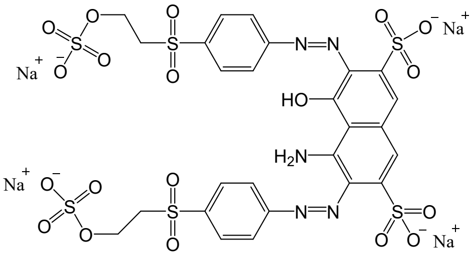 Reactive Black-5 (RB-5) Molecular weight: 991.8	Negative	2.9×0.85
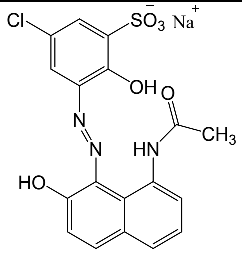 Omega chrome black blue G (OG) Molecular weight: 457.8	Negative	
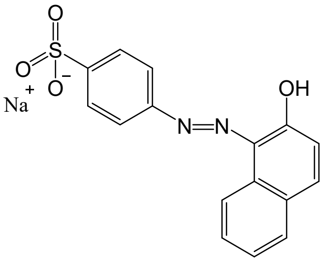 Acid orange 7 (AO-7) Molecular weight: 350.3	Negative	

Table S1. The molecular structure, molecular weight, charge, and size of the dyes.

Synthesis of poly(methyl methacrylate)-*co*-poly(vinyl benzyl chloride) (PMMA-*co*-PVBC)

Free radical copolymerization was used to synthesized PMMA-*co*-PVBC copolymer as follows. In a round-bottom flask with a bar magnet, we took purified MMA (56 g, 0.56 mol), VBC (24 g, 0.157 mol) and 320 mL of DMF. Then into the admixture 0.4 g of AIBN was added. After 10 minutes of N_2 purging in the reaction mixture, rubber septum was used to cap the flask and it was fastened with copper wire. The reaction mixture was agitated at 70°C for 8 h. Excess isopropanol was used to precipitate the copolymer in order to eliminate unreacted monomers. The precipitation process was repeated by re-dissolving the solid mass in DMF and reprecipitating it in isopropanol. Lastly, the copolymer was dried for 48 hours at 70°C in a vacuum oven.[4] This copolymer was directly employed for preparation of blend membrane.

Synthesis of quaternized poly(vinyl imidazole) (PVIm-Me)

Firstly, the vinyl imidazole (VIm) monomer was passed through basic alumina column twice and stored at -20 ^{o}C. PVIm was synthesized as follows. VIm (5 g), DMF (10 mL) and AIBN (0.02 g) were taken into a round bottom flask. After that, the solution was nitrogen-purged for ten minutes. After being sealed with a rubber septum, the flask was submerged in an oil bath heated to 70 °C under stirring for eight hours. The solution was then precipitated in acetone after DMF was reduced to one-third of its original volume under lower pressure. The resulting precipitated polymer was re-precipitated in acetone after being dissolved in methanol. The polymer was vacuum-dried completely. Further, the obtained PVIm was quaternized as follows. After dissolving PVIm (5 g, or 0.053 mol of VIm unit) in 20 mL of DMF, 15 g of methyl iodide (0.106 mol) was added to the mixture. The reaction mixture was left to agitate at room temperature for 24 h. The reaction mixture was concentrated, then precipitated into acetone. The resulting polymer was extensively dried in a rotary evaporator to produce PVIm-Me.[5]

Synthesis of poly(styrene sodium)sulfonate ($PStSO_3Na$)

$PStSO_3Na$ was synthesised as follows. Briefly, $StSO_3Na$ (5 g) was dissolved in 15 mL of deionized water before adding the initiator ACPA (0.02 g) to the solution. The solution was purged with nitrogen for 10 minutes. The polymerization was carried out for 8 h at 70 °C. The polymer was precipitated in THF to eliminate any unreacted monomers. The process was repeated twice. The separated polymer was dried under low pressure and stored in a desiccator.[5]

Preparation of base membrane substrate

A cationic base membrane (MWCO=4x10^5 g mol^{-1}) was prepared as follows.[4,5] Briefly, a casting solution containing PVDF (8.9 g), PVP (4.3 g, M_n=3.6x10^5 g mol^{-1}) and PMMA-*co*-PVBC (3.9 g) was prepared in DMF (83 g). The casting solution was kept overnight to remove the air bubbles. The solution was then casted on a non-woven fabric (30 cm x 10 m, Awa Japan) by a blade casting machine. The contact time of the casted solution to the water gelation bath was 6 s. The obtained roll of the membrane (PVDF-0) was thoroughly washed with deionized water. Further, dipped into a 500 mL solution of trimethylamine (5% v v^{-1}) in water (pH 9). The reaction was performed in a glass cylinder sealed with a stopper for 24 h at ~27 °C. After that, the membrane role was dipped in water to get rid of the unreacted amine. This membrane was used as the base substrate for the LbL assembly.

Determination of permeate flux, MWCO, pore size of the membranes and evaluation of dye rejection efficacy and fractionation of dye and salt

The cross-flow filtration system equipped with four interconnected SS316 cells (14.5 cm^2 effective area), control needle valve, pressure-gauge, and centrifugal pressure pump (flow rate=40-45 L h^{-1}) were used for the filtration operation and determination of performance of the membranes. In order to obtain steady permeate flux, the membranes were first pre-pressurized with pure water at an applied pressure of 2 bar for 3 h. The pure water flux (J_w) of the membranes were then determined at applied pressure of 1.38 bar using following equation:

$$J_w = \frac{V}{At} \qquad (S1)$$

where V is the permeate water volume, A is the membrane area (m^2) and t is the permeate time (h). The applied pressure was also varied. Averages of eight membrane swatches were taken.[5,6]

The molecular weight cut-off (MWCO) of the membranes was determined by permeating PEG solution (500 mg L^{-1}) of different molecular weight. The membranes were first pre-pressurized with pure water at an applied pressure of 2 bar for 3 h in a re-circulation mode. Further, PEG solutions of different molecular weight were permeated one by one at an applied pressure 1.38 bar. The samples were collected after permeation for 10 min for 20 min duration to evaluate the rejection (equation S2):

$$R = \left(1 - \frac{C_p}{C_f}\right) \times 100\% \qquad (S2)$$

where C_f and C_p are the concentrations of PEG in the feed solution and permeate water respectively. The C_p and C_f were measured by the GPC experiments. Plots of rejection vs. M_n of PEG gave the MWCO values (at 90% rejection) of the membranes. The Stokes diameter of PEG and PEO samples were used for the determination of MWCO of the membranes (equations S3 and S4).

$$For\ PEG: ds = 33.46 \times 10^{-12} \times Mn^{0.557} \qquad (S3)$$

$$For\ PEO: ds = 20.88 \times 10^{-12} \times Mn^{0.587} \qquad (S4)$$

A log-normal plots of PEG rejections and Stokes diameter (d_s) of the PEG gave the mean pore diameter (μ_p) at 50% rejection (R) and the geometric standard deviation (σ_p), the ratio of d_s at R=84.13% over that at R=50%. The pore size distributions of the membranes were determined by the following probability density function.[7]

$$\frac{dR(d_p)}{dd_p} = \frac{1}{d_p \ln \sigma_p \sqrt{2\pi}} \exp\left[-\frac{(\ln d_p - \ln \mu_p)^2}{2(\ln \sigma_p)^2}\right] \qquad (S5)$$

Separation of dye and salt

The membranes were pre-compacted with pure water at a higher pressure to obtain steady permeate flux before performing separation experiments. All the separation experiments were undertaken in a crossflow filtration system consisting of four stainless steel cells connected in a series, each cell having effective area of 14.5 cm^2. Individual salt (NaCl, Na_2SO_4 and $MgCl_2$) rejection experiment was performed with feeds containing varying concentration of salts (2-50 g L^{-1}) at an applied pressure of 2.76 bar while individual dye rejection experiment was performed using feeds having varying concentration of dyes (0.02-1 g L^{-1}) at an applied pressure of 1.38 bar. The selective separation of dye and salt was performed using feeds containing mixture of dye (1 g L^{-1}) and salt (NaCl or Na_2SO_4, 50 g L^{-1}) except in the feed containing CR (1 g L^{-1}), the salt (NaCl/Na_2SO_4) concentration was 20 g L^{-1} at an applied pressure of 1.38 bar. The dye rejection was ascertained by UV-Visible analysis (UV-2700, Shimadzu, Japan) while the rejection of salt was quantified using conductivity data (Eutech PC2700). An ion chromatography analysis was performed to confirmed the salt rejection. The separation factor (S) was determined by the following equation:[6,7]

$$Salt\ to\ dye\ separation\ factor = \frac{100 - salt\ rejection}{100 - dye\ rejection} \quad (S6)$$

Determination of dye antifouling property

To ensure a steady permeate flux, the membrane swatches were first pre-pressurized. The pure water flux was then measured at 1.38 bar over time. The water was replaced with a dye (DR-80, 1 g L^{-1}) solution, and the dye rejection and permeate flux were determined over time. After a period of filtering, the membrane swatches were washed with water thoroughly for 10 minutes in the same cross-flow setup. Again, the dye solution was permeated. This process was repeated thrice. The dye solution was changed with a dye (DR-80, 1 g L^{-1}) + salt (NaCl, 50 g L^{-1}) solution to test the effect of salt on membrane fouling. The antifouling experiment was carried out for three cycles of 20 h each. The flux recovery ratio (FRR) and flux reduction (FR) values were calculated using the following equations:

$$FRR = \frac{J_c}{J_w} \times 100\% \quad (S7)$$

$$FR = \frac{J_w - J_t}{J_w} \times 100\% \quad (S8)$$

where J_w and J_c represents the membrane pure water fluxes prior to and following the antifouling test respectively. J_c was determined after washing the membrane with water. J_t represents the membrane flux at any given time during the antifouling experiment.

Fractionation of dye/salt by diafiltration operation

According to the standardization experiments, Mem-PEC3 membrane demonstrated good salt to dye separation efficacy. Thus, Mem-PEC3 membrane after pre-compaction subjected to the diafiltration operation using feed solutions (500 ml) containing CR dye (1 g L^{-1}) and salt (NaCl or Na_2SO_4, 20 g L^{-1}) in a crossflow filtration system as described above. The diafiltration operation were conducted in a batch mode to explore recovery ability of Mem-PEC3.[8] In batch mode, the feed volume was initially 500 ml from which 250 ml of permeate was collected (50% water recovery) and then 250 ml of pure water was added to makeup the feed volume. As previously mentioned, the dye and salt concentrations in the feed and permeate were measured with each diavolume.

Effect of salt on the PEC

The PEC remained in precipitated state at presence of 4 M NaCl (Fig. S1A). This indicates no complete disintegration of the PE particles. However, loosening of the structure by fraction of ion pair disruption through extrinsic compensation in the PEC may be possible. This is evident by the lowering of salt rejection with increasing salt concentration. The lowering of salt rejection with increasing feed concentration is due to the both charge shielding and ion pair disintegration as discussed above. The charge shielding effect is well reflected in zeta potential values of the PECs (Fig. 1, in the main text). The UV-Visible analysis also indicates stability of the PEC in the presence of NaCl (Fig. S1B). However, KBr is a strong salt and it dissociate the PEs ion pair. This is well known behavior of KBr (main text).

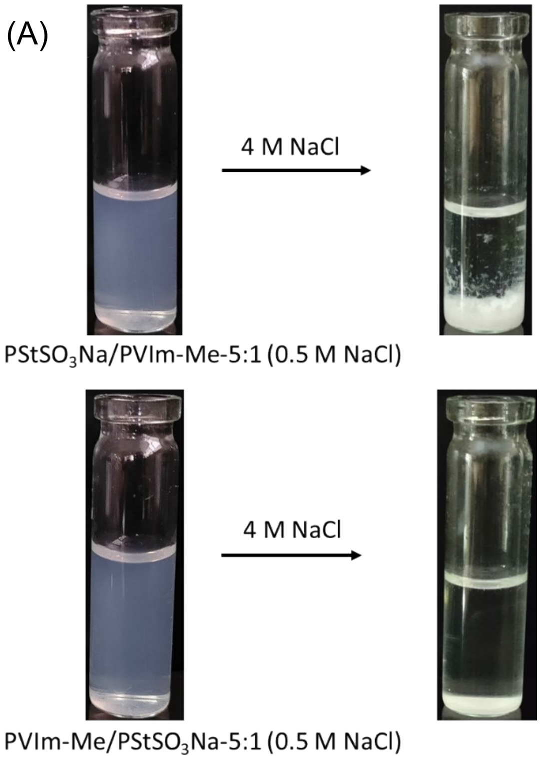

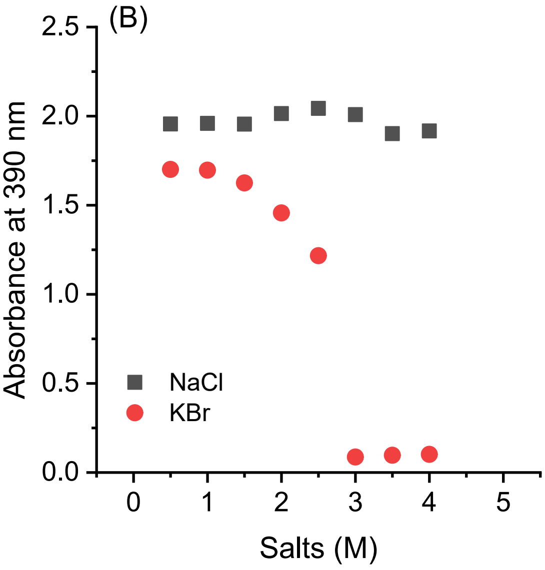

Fig. S1 (A) Digital photographs showing stability of the PECs in presence of excess salt. (B) Stability of the representative PStSO$_3$Na/PVIm-Me-5:1 PEC in presence of different salts.

Effect of concentration of salt on the particle size distribution of the PECs

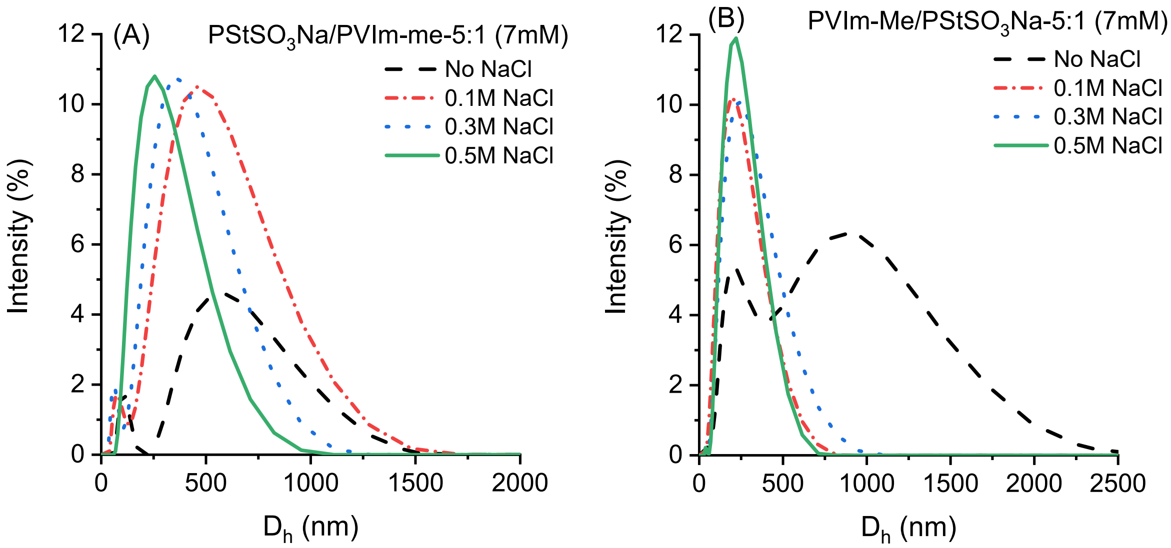

Fig. S2 Variation of particle size distribution of the PEC with the variation of NaCl concentration. The PECs were prepared in the presence of different concentration of NaCl. The freshly prepared PECs were immediately used for the DLS analysis.

Evaluation of the dispersion stability of the non-stoichiometric PECs

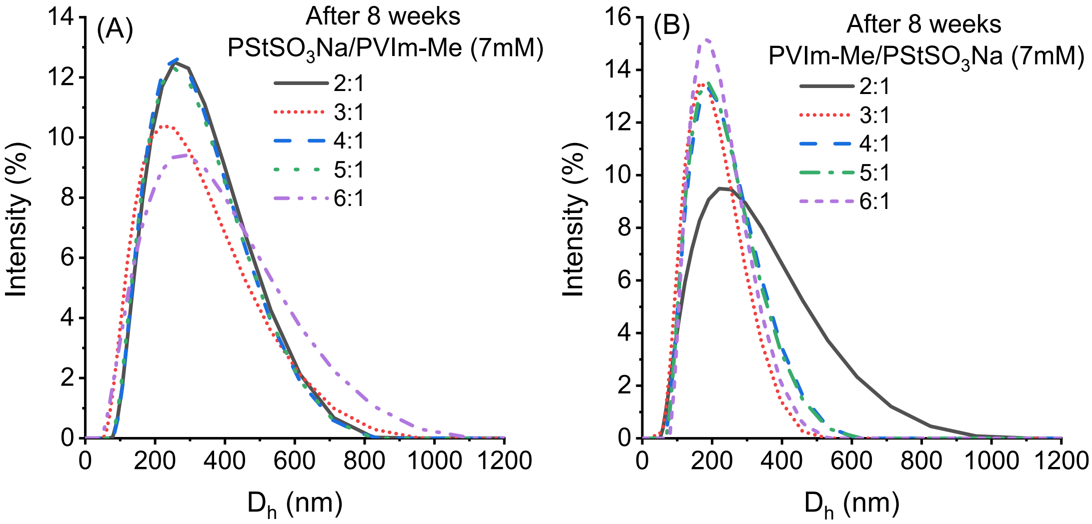

Fig. S3 (A and B) DLS curves of the PECs recorded after the eight weeks of storage at room temperature (without stirring). The PECs were prepared by varying the ratio (mol/mol, monomer unit equivalent) of the PEs in the presence of constant (0.5 M) NaCl.

Effect of PE concentration on the size of the PECs

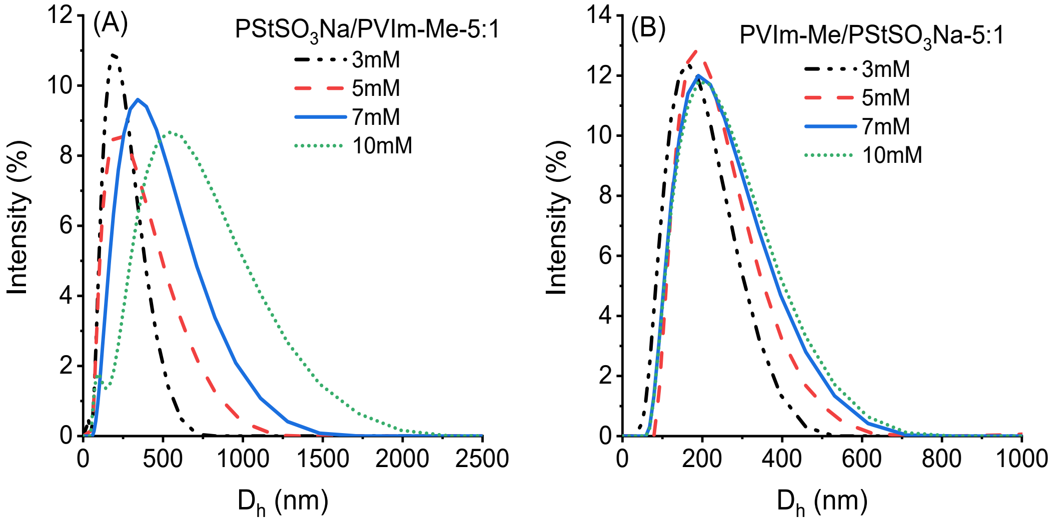

Fig. S4 (A and B) DLS size distribution profiles of the PECs. The PECs were prepared at different concentration of PEs (fixed stoichiometry, 5:1). The NaCl concentration was 0.5 M.

Effect of centrifugation on the size of PECs

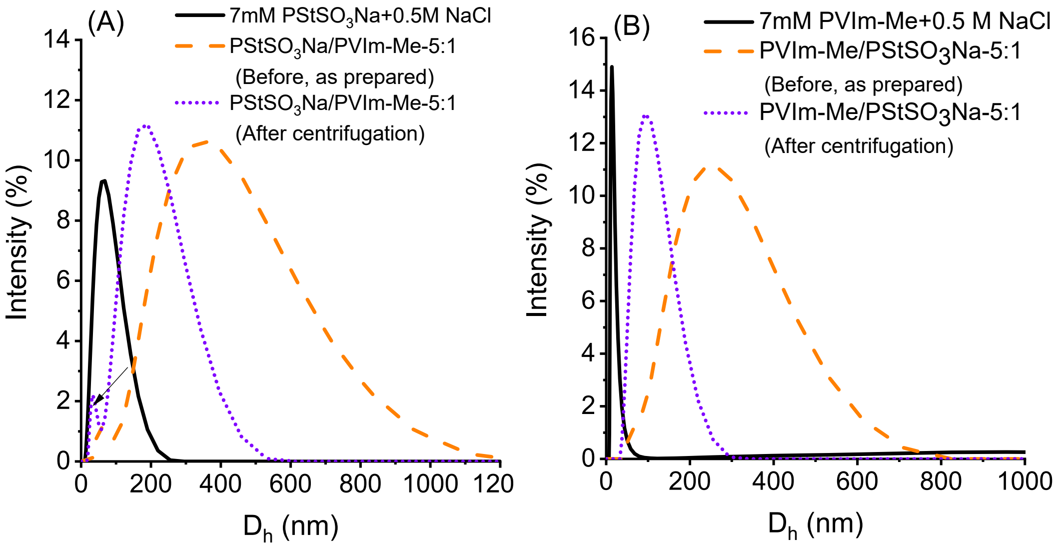

Fig. S5 DLS size distribution profiles of the representative (A) PStSO$_3$Na PE, and PStSO$_3$Na/PVIm-Me-5:1 PEC before and after centrifugation and (B) PVIm-Me PE, and PVIm-Me/ PStSO$_3$Na-5:1 PEC before and after centrifugation.

Evaluation of effect of type of PEC on the performance of LbL assembled membrane (total three layers)

The charge of the PECs depends on the PEs stoichiometry. The PECs formed at PEs stoichiometry of 5:1 to 6:1 and each PE concentration of about 7 mM are found to be suitable for LbL assembly. The membrane formed by the LbL assembly of the anionic PStSO$_3$Na/PVIm-Me-5:1 and cationic PVIm-Me/PStSO$_3$Na-5:1 exhibited good rejection of CR, RB and RB-5 (Fig. S6).

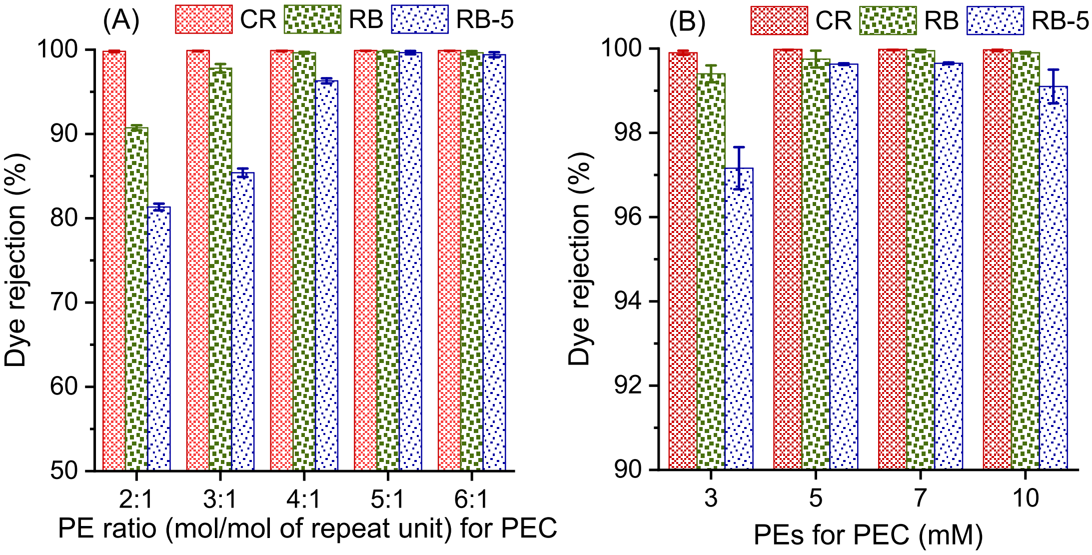

Fig. S6 (A) Composition of PECs (stoichiometry) on the dye rejection performance of the LbL assembled membranes. The PECs were prepared at fixed concentration (7 mM) of PEs and different stoichiometry of the PEs. (B) Effect of concentration of the PEs used for the preparation of PECs (5:1 mol/mol of repeat unit) on the dye rejection performance of the LbL assembled membranes (total three layers). The oppositely charged PECs were PStSO$_3$Na/PVIm-Me and PVIm-Me/PStSO$_3$Na for the LbL assembly to fabricate membranes.

Surface SEM images of LbL self-assembled membranes and determination of thickness of the isolated layers of the membranes

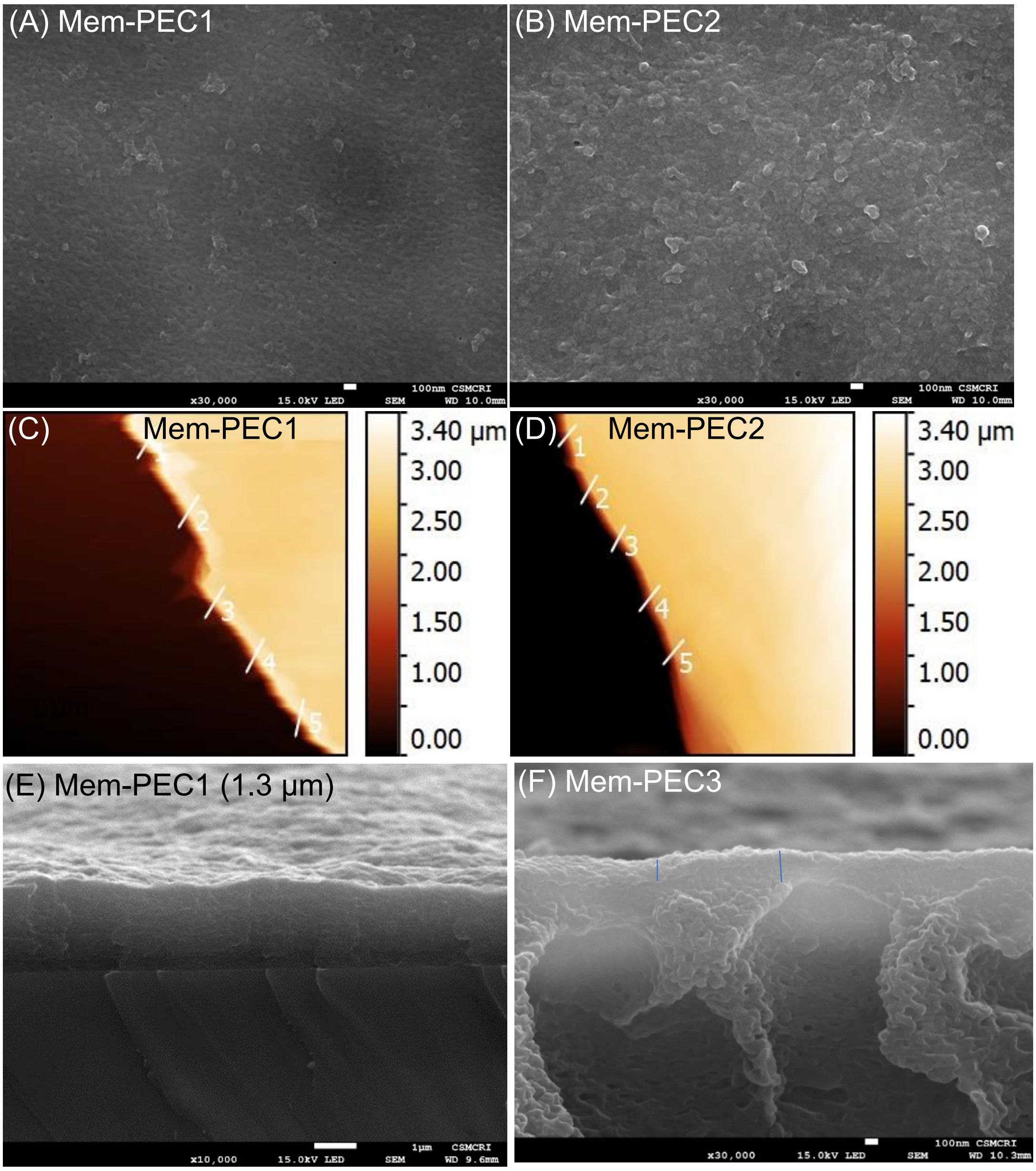

Fig. S7 (A and B) Surface SEM images (x30 k magnification) of representative membranes. (C and D) AFM thickness analysis of the isolated layers of the representative membranes. (E) Cross-sectional SEM image of the isolated layer of Mem-PEC1 membrane. The PEC layer was isolated on silicon wafer by leaching the base substrate with DMF for thickness determination. (F) Cross-sectional SEM image of the Mem-PEC3. The as prepared membrane was frozen in liquid nitrogen and then fractured for the cross-sectional SEM analysis.

High magnification SEM images of base substrate and representative membranes

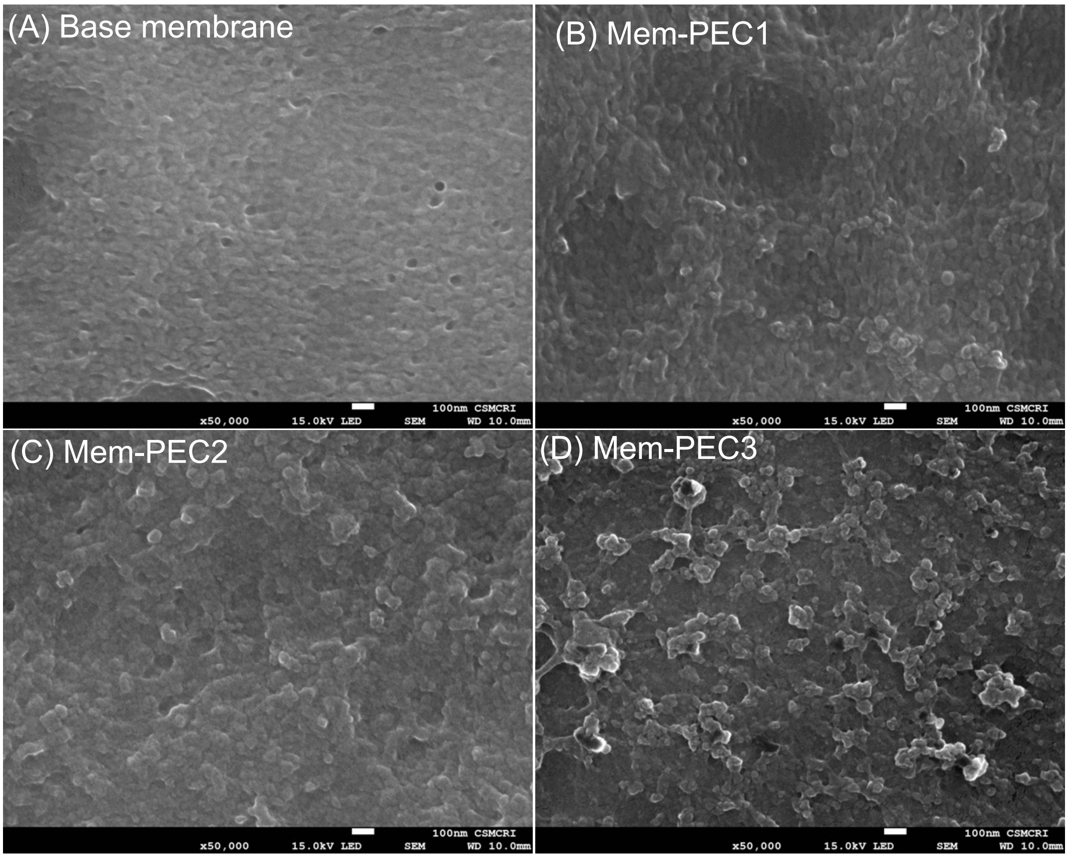

Fig. S8 (A-D) Surface SEM images (x50 k magnification) of base substrate and representative membranes.

MWCO and pore size distribution of base substrate and Effect of pH 12 treatment on MWCO and pore size distribution of Mem-PEC3 membrane

The MWCO and pore size distribution of the Mem-PEC3 was determined before and after treatment at pH 12 (Fig. S9C and D). The PECs contain ion pair. The ion pair are generated during LbL assembly of the oppositely charged PECs. This PECs are formed by the strong electrostatic attraction between the oppositely charged PEs. The change of MWCO and pore size distribution is negligible after treatment at pH-12.

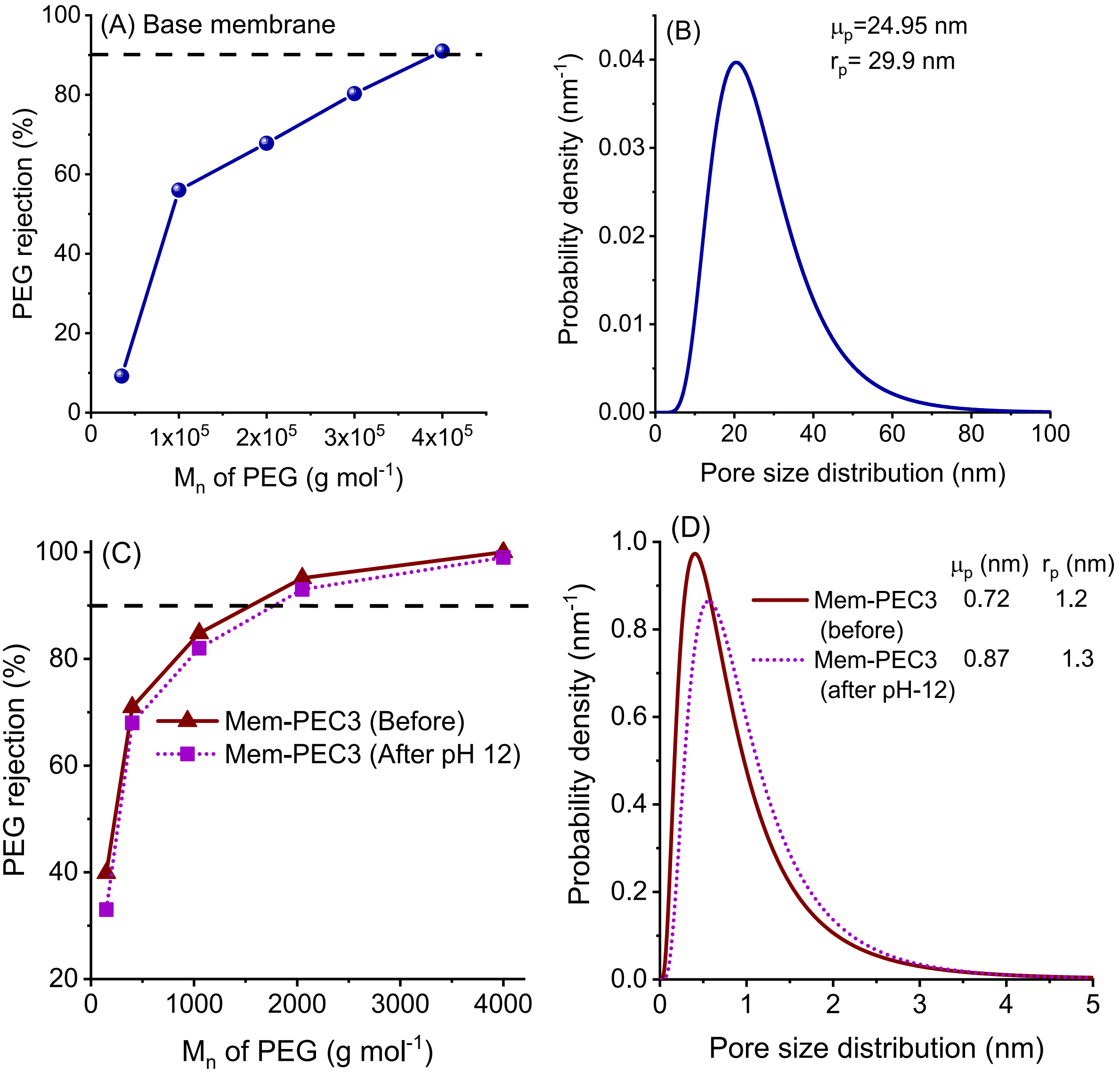

Fig. S9 (A and B) MWCO and pore size distribution of base substrate. (C and D) MWCO and pore size distribution of Mem-PEC3 membrane before (as prepared) and after treatment at pH 12. The pH stability of the membrane was verified by permeating water of pH 12 for 12 h. After that the MWCO and pore size distribution of the membrane was evaluated.

ATR-IR analysis and N1s core level spectra of the membranes

The ATR-IR analysis was performed to determine the relative attachment of the PECs on the Mem-PEC1, Mem-PEC2 and Mem-PEC3. The PECs LbL assembled membranes show bands at 1035 cm^{-1} and 1010 cm^{-1} due to the S=O stretching vibration. The PECs contain $PStSO_3Na$. Obviously, base membrane does not show this band (Fig. S10A and B). The relative adsorption of the PECs was determined by plotting the I_{1035} to I_{880} ratio vs. layer number. Herein, I_{1035} and I_{880} are the intensity of bands at 1035 cm^{-1} and 880 cm^{-1} respectively. The later band is ascribed to the C-F stretching vibration of PVDF base substrate. The IR intensity of the band at 880 cm^{-1} changes insignificantly unless the thickness of LbL self-assembly layer is high or exceeds the penetration depth of evanescent IR wave.[9] The penetration depth of the ATR-IR is about 1 μm. This consideration is based on the thin layer formation, which was evident from the cross-sectional SEM analysis and model LbL assembly on silicon wafer. Hence, the band at 880 cm^{-1} is considered as reference band. The I_{1035} to I_{880} ratio increases with increasing layer number. The anionic PEC contain free $-SO_3Na$ while the cationic PEC contains $-SO_3$ moieties in the form of ion pair. The calculated I_{1035}/I_{880} for the third layer is close to the calculated value for first layer (subtracting the value of second layer from third layer) (Fig. S10C). In contrast, the adsorption of the anionic PEs in the first layer is greater than the higher layer for the LbL assembly of the uncomplexed PEs.[5,10] Adsorption of PE and PEC is thus different on the porous base substrate. The size of the majority of the PECs is bigger than the pore size of the base membrane substrate. The electrostatic adsorption of the anionic PEC occurs predominantly on the surface rather than inside pores of the base substrate. On the other hand, PE attained coil conformation in the presence of salt. The smaller size and higher diffusion of the precursor PE as compared to that of the PEC facilitates the attachment of the former inside the pores and pore wall during first layer formation.

N1s core level spectra of the membranes show peak for CN^+ with enhanced fractional area from base substrate to Mem-PEC3 (Fig. S10D-G). The PECs contain cationic PE in the free or neutralized state. The base substrate contains quaternized amine and hence showed the peak for the CN^+.

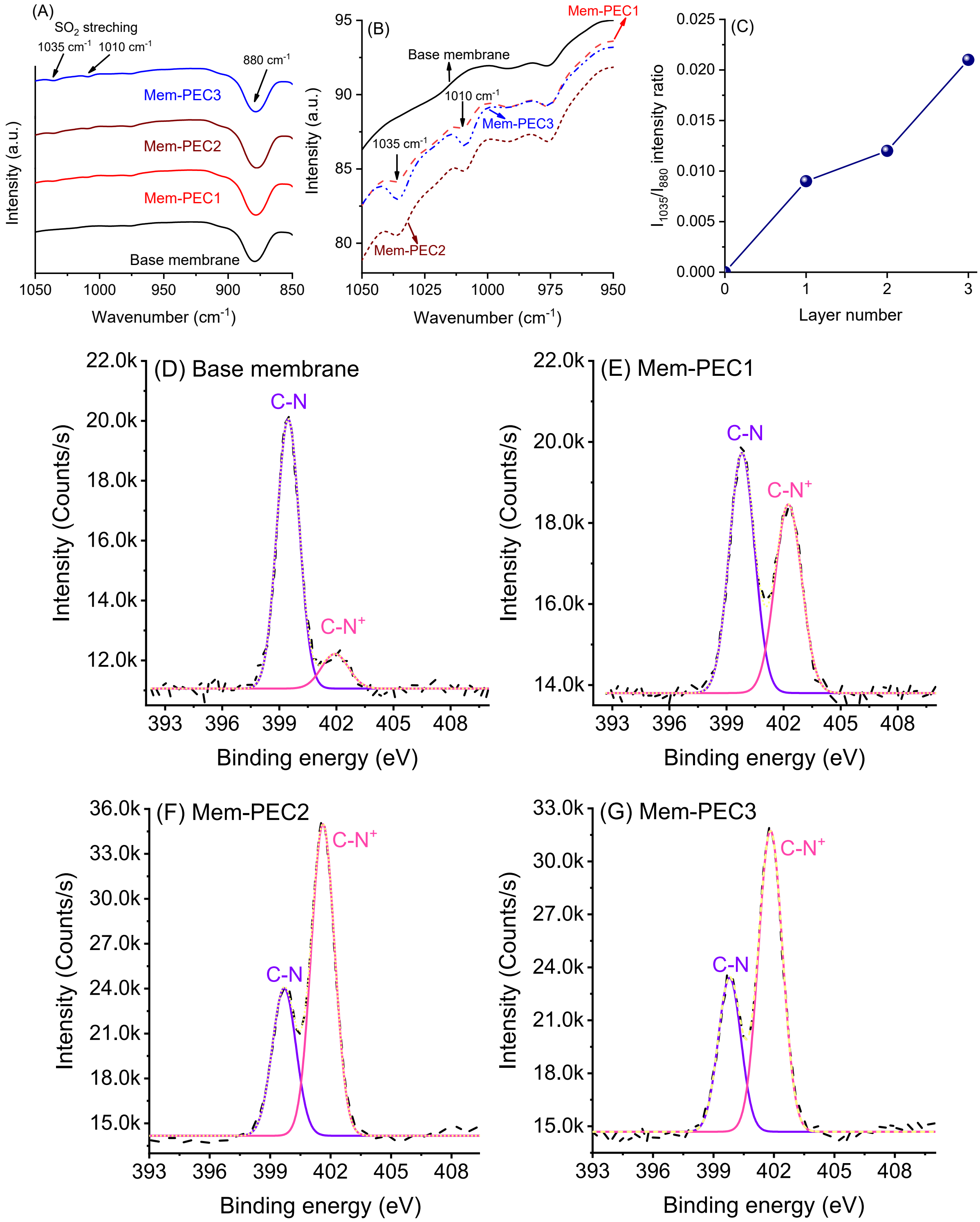

Fig. S10 (A) ATR-IR, (B) extended scale ATR-IR spectra of the membranes. (C) Plot of I_{1035}/I_{880} (Averages of 05 spots) vs. layer number. (D-G) N1s core level spectra of the membranes.

Effect of salt concentration on the rejection efficacy of the membrane

The salt rejection by the Mem-PEC3 follows the order for the salts, Na_2SO_4>$MgCl_2$>NaCl. The membrane contains excess -SO_3Na at the surface which enhances the Donnan exclusion with similarly charged SO_3^{2-} while electrostatic attraction is facilitated with Mg^{2+} (Fig. S11). However, the salt rejection efficacy decreases with increasing salt concentration. This is usually observed for the LbL assemble membranes. High salt concentration causes membrane charge shielding as a result, the electrostatic repulsion with the similarly charged ions decreases. However, the rejection of Mg^{2+} should not decrease if only electrostatic force is considered. This indicates that the other than electrostatic force, swelling of the LbL assembled layer in the presence of high salt concentration may also be operative. Swelling of layers of the oppositely charged PEs is a common problem in the separation applications.[11] Not only LbL assembled layer, other membranes also showed salt induced pore enlargement.[12,13] Nevertheless, fortunately, the aggregate size of dye is bigger than the pore size of the membrane. The aggregate size and the extent of aggregation further increase in the presence of salt. Thus, membrane swelling and pore enlargement is not reflected during the dye interception herein.[8,14] Indeed, dye rejection slightly increased and salt rejection decreased with increasing salt concentration during fractionation of dye+salt mixture. The salt effect is not permanent. The salt rejection again regained at low salt concentration.

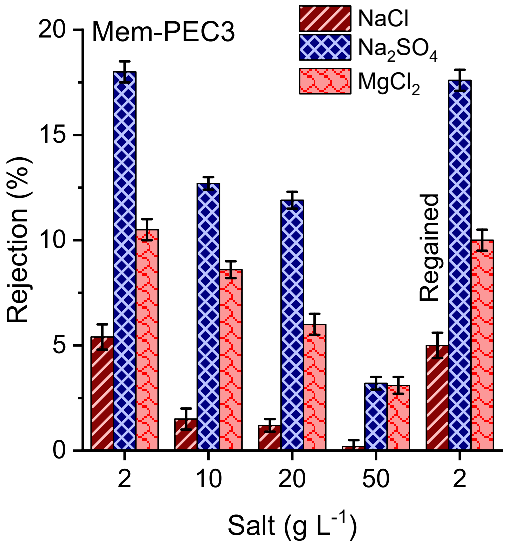

Fig. S11 Change of salt rejection efficacy of representative Mem-PEC3 membrane with increasing feed concentration. The salt rejection again regained at salt concentration of 2 g L^{-1}. The applied pressure was kept at 2.75 bar as the dye rejection was performed at an applied pressure of 1.38 bar. The salt rejection may be altered at higher applied pressure.

Effect of concentration of dye on the membrane rejection in the presence of salt (50 g L^{-1})

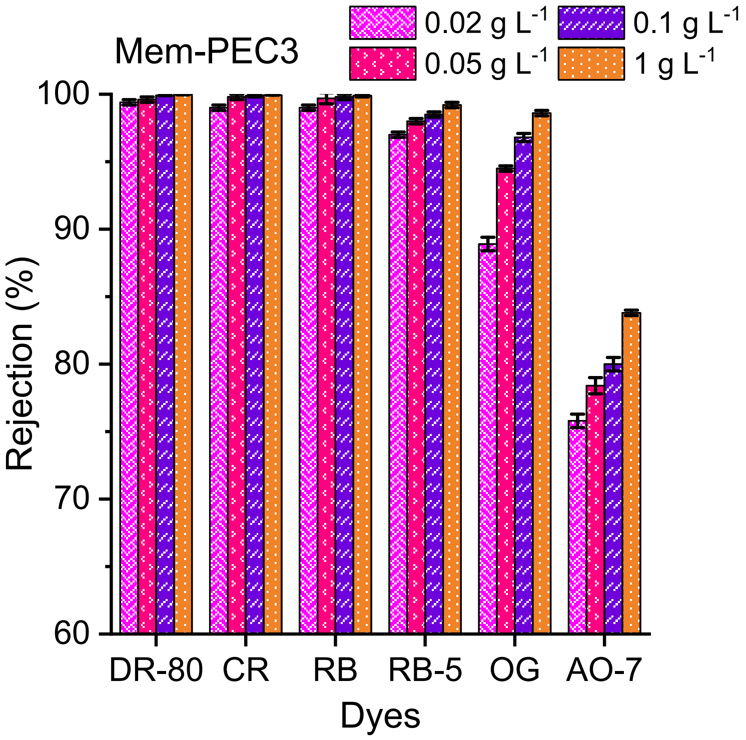

Fig. S12 Effect of concentration of dye (except CR) in presence of NaCl (50 g L^{-1}) on the Mem-PEC3 rejection efficacy. The NaCl concentration was 20 gL^{-1} in the CR solution. The NaCl rejection is about 3%.

Effect of salt on the DR-80 and RB rejection

The DR-80 rejection showing increasing trend in the presence of NaCl. It may be seen that the UV-Visible spectra of the DR-80 show a hump at 523 nm in the presence of salt due to the enhanced aggregate formation. The enhanced aggregation of the dye in the presence of salt enhanced the dye rejection. Though, pore swelling may be occurred in the presence of salt but not reflected as the size of dye aggregate is larger than the effective pore size of the membrane.

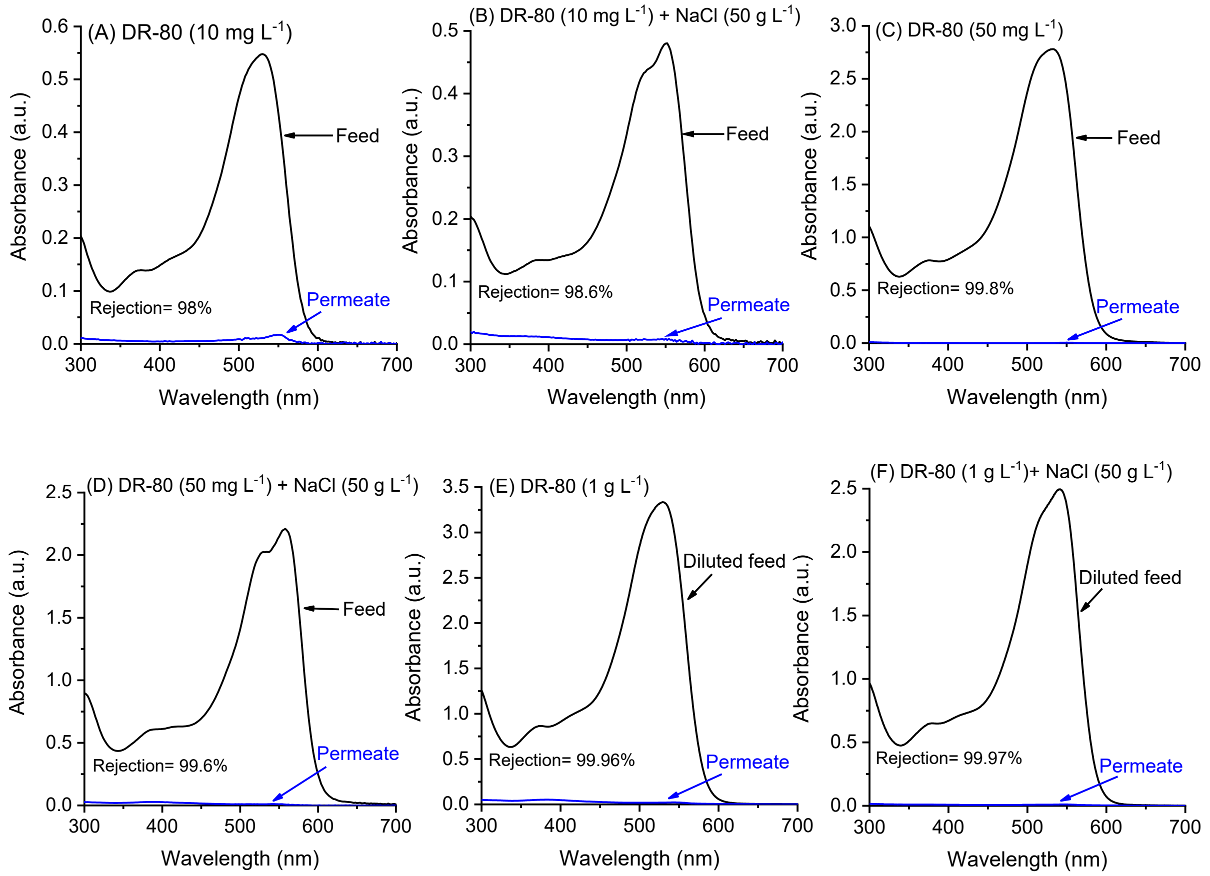

Fig. S13 UV-Visible spectra of feed solution and permeates through the Mem-PEC3 membrane at different concentration of dye (DR-80) and effect salt (NaCl) on the rejection efficacy.

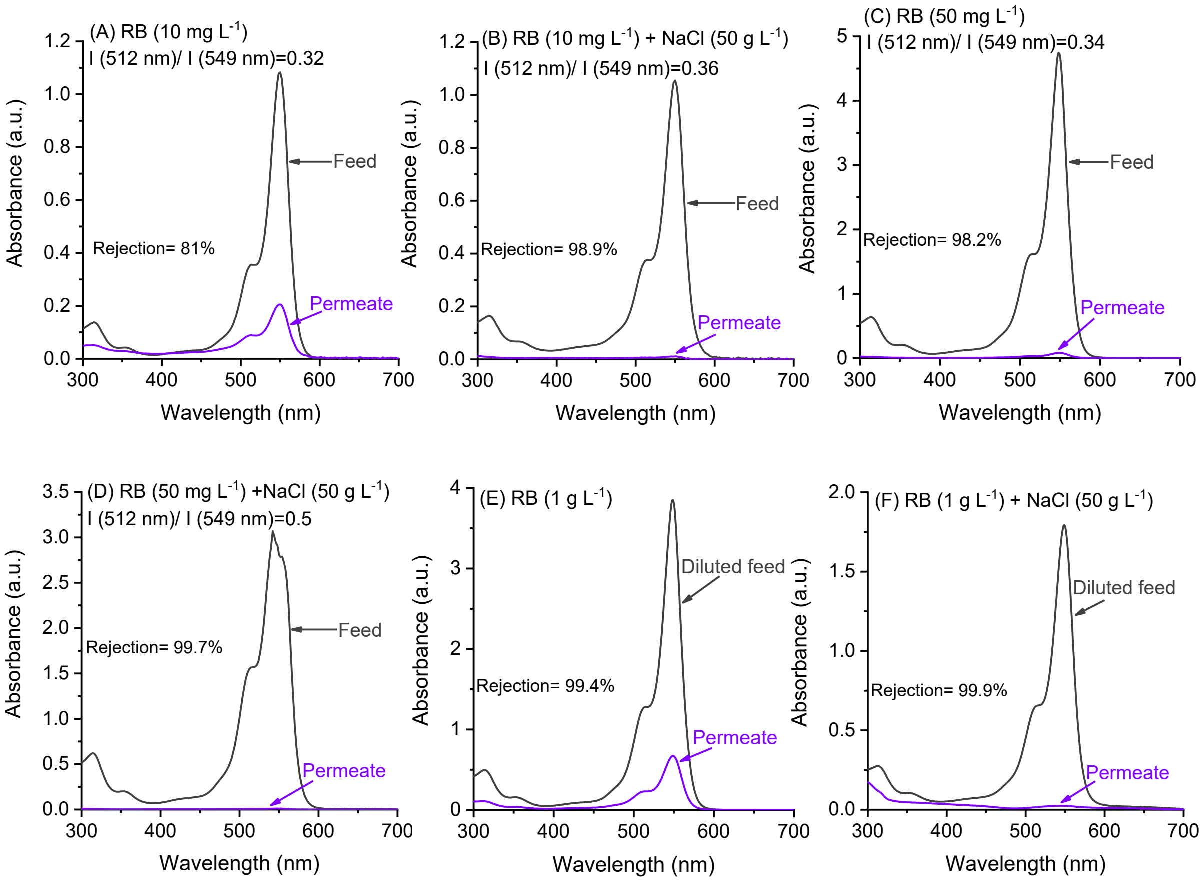

Fig. S14 UV-Visible spectra of feed solution and permeates through the Mem-PEC3 membrane at different concentration of dye (RB) and effect of presence of salt (NaCl) on rejection efficacy.

Effect of concentration of salt on the dye rejection and salt to dye separation factor of Mem-PEC3 membrane

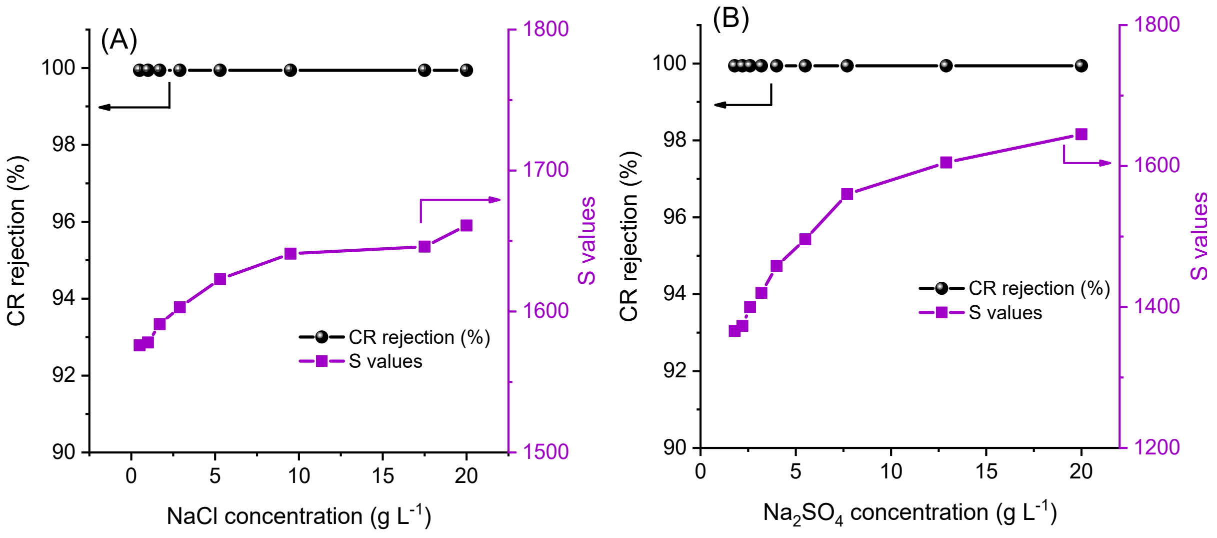

Fig. S15 CR rejection and salt (NaCl or Na_2SO_4) to CR separation factor (S) of the Mem-PEC3 membrane with variation of salt concentration in the feed. The CR concentration was 1 g L^{-1}. The separation experiments were conducted at an applied pressure of 1.38 bar.

Fractionation of salt and CR by batch diafiltration operation

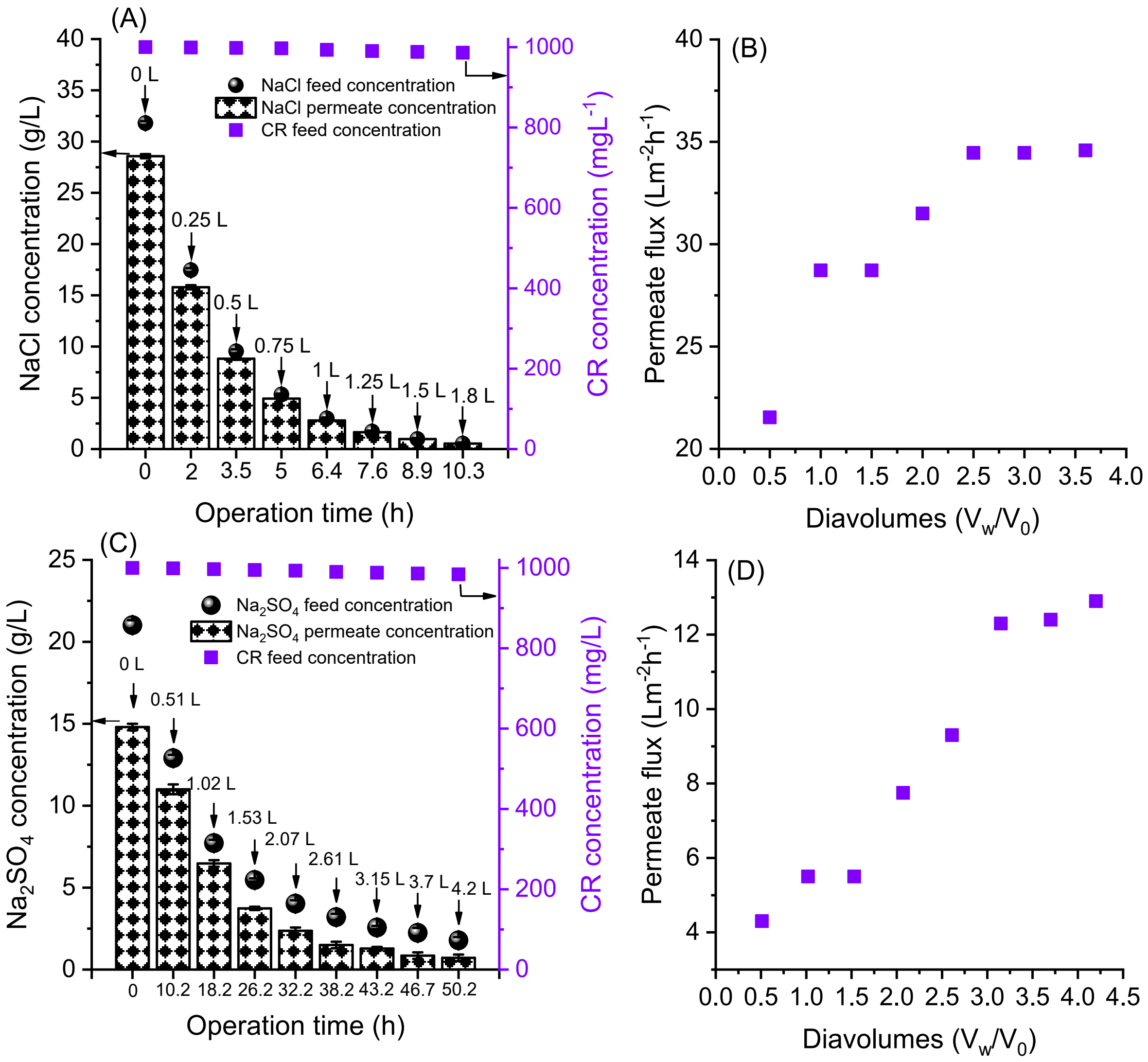

Fig. S16 Fractionation of (A) NaCl+CR and (C) Na_2SO_4+CR mixtures using Mem-PEC3 membrane and (B and D) permeate flux of Mem-PEC3 membrane during diafiltration. The applied pressure was 1.38 bar during the operations. V_w/V_0 is ratio of initial feed volume and the water added each time.

Comparison of RB-5 rejection performance of the membranes prepared by parent PEs and PECs

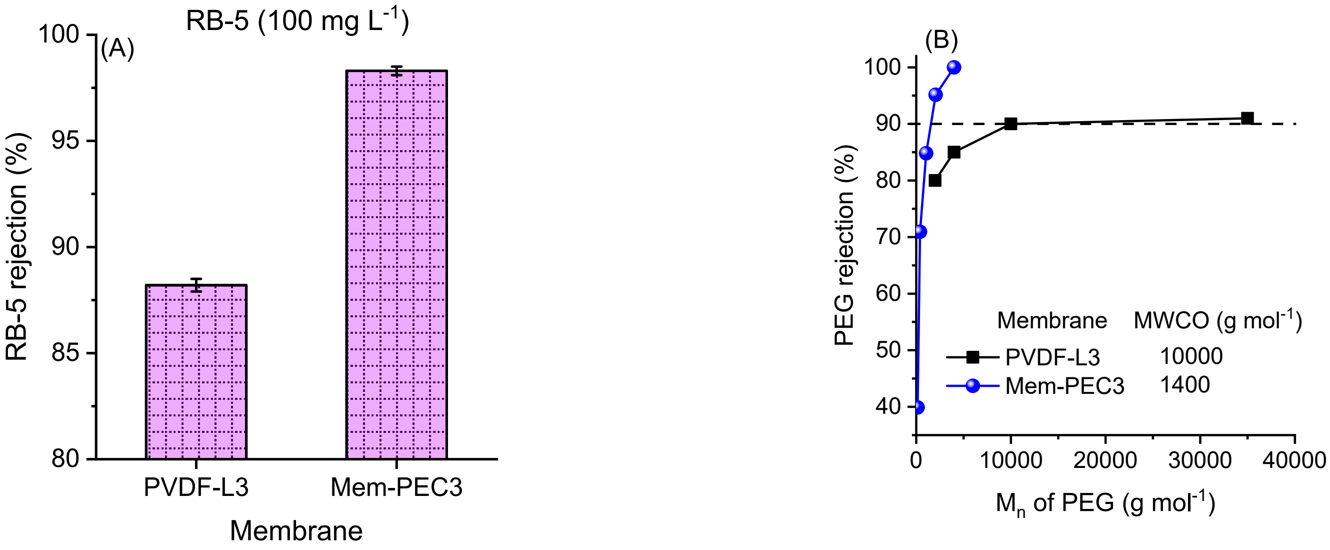

Fig. S17 Comparison of (A) dye rejection performance and (B) MWCO of the membranes (total three layers) prepared by uncomplexed PEs (20 mM each) and PEC (7 mM) based conventional LbL self-assembly.

References

1. L. Huang, S. Huang, S. R. Venna and H. Lin, *Environ. Sci. Technol.,* 2018, **52**, 12649-12655.
2. P. Wu and M. Imai, *Desalin. Water Treat.*, 2013, **51**, 5237-5247.
3. K. J. Hwang, J. Y. Park, Y. J. Kim, G. Kim, C. Choi, S. Jin and W. G. Shim, *Sep. Sci. Technol.,* 2015, **50**, 1757-1767.
4. D. V. Bhalani, A. Bera, A. K. S. Chandel, S. B. Kumar and S. K. Jewrajka, *ACS Appl. Mater. Interfaces,* 2017**, 9**, 3102-3112.
5. U. S. Joshi, D. V. Bhalani, A. Chaudhary and S. K. Jewrajka, *J. Membr. Sci.,* 2022**, 641**, 119908.
6. U. S. Joshi, Anuradha and S. K. Jewrajka, *J. Membr. Sci.*, 2023, **669**, 121286.
7. J. Lin, W. Ye, M. C. Baltaru, Y. P. Tang, N. J. Bernstein, P. Gao, S. Balta, M. Vlad, A. Volodin, A. Sotto, P. Luis, A. L. Zydney and B. Van der Bruggen, *J. Membr. Sci.,* 2016, **514**, 217-228.
8. R. Zhao, Y. Li, Y. Mao, G. Li, T. Croes, J. Zhu, X. You, A. Volodin, J. Zheng and B. Van der Bruggen, *Environ. Sci. Technol.,* 2022, **56**, 17998-18007.
9. R. Bernstein, S. Belfer and V. Freger, *Langmuir,* 2010, **26**, 12358-12365.
10. U. S. Joshi, S. Samanta and S. K. Jewrajka, *ACS Appl. Mater. Interfaces,* 2024, **16** 32748−32761.
11. J. Chen, S. Xu, C. Y. Tang, B. Hu, B. Tokay and T. He, *Desalination*, 2023, **555**, 116520.
12. M. Nilsson, G. Trägårdh and K. Östergren, *J. Membr. Sci.*, 2008, **312**, 97-106.
13. J. Luo and Y. Wan, *J. Membr. Sci.,* 2011, **372**, 145-153.
14. J. Lin, W. Ye, H. Zeng, H. Yang, J. Shen, S. Darvishmanesh, P. Luis, A. Sotto and B. Van der Bruggen, *J. Membr. Sci.,* 2015, **477**, 183-193.